

Received August 16, 2019; reviewed; accepted October 16, 2019

Simulations of a multicomponent mixture in the reflux classifier to demonstrate the effect of dispersion coefficient on its internal state

Naveedul Hasan Syed, Naseer Ahmed Khan, Muddasar Habib

Department of Chemical Engineering, University of Engineering and Technology Peshawar Pakistan

Corresponding author: syednaveed@uetpeshawar.edu.pk (Naveedul Hasan Syed)

Abstract: In this study, influence of the dispersion coefficient on the internal state of a multicomponent mixture comprising 35 types of particle species with five different sizes ranging $-2.0+0.25$ mm and seven different densities, 1400 to 2000 kg/m³, in a reflux classifier under continuous process conditions is presented. Simulations were performed to study the effect of dispersion coefficient on the separation density, D_{50} , separation efficiency, E_p , and solid volume fraction of the multicomponent mixture. The simulation results provided a good agreement with the published experimental results of the reflux classifier, operated at full scale in 2005, for a relatively high value of the dispersion coefficient, 0.0030 m²/s, and a relatively small value of the dispersion, 0.00030 m²/s, in the fluidization and inclined sections of the device, respectively. Moreover, different fixed values of the dispersion coefficient and a published proposed model of the dispersion coefficient were incorporated in the model to examine variations in the system and were compared with the validated simulation results. It was found that the selected values of the dispersion coefficient had not much effect on the D_{50} values. However, the E_p values changed significantly with changes in the dispersion coefficient values. The smaller values of the dispersion coefficient provided lower values of the E_p that did not match well with the validated simulation results. Furthermore, the variations in the total solid volume fraction within the reflux classifier for different values of the dispersion coefficient has been demonstrated.

Keywords: continuum model, dispersion flux, ecart probable error, segregation, slip velocity

1. Introduction

The complex process of fluidization has a wide range of applications, e.g. coal processing, mineral processing, food technology, wastewater treatment and bio-solubilization of coal particles, etc. over other configurations due to several advantages such as easy solids handling, efficient solids mixing, high mass and heat transfer rates (Di Felice, 1995). The utilization of the fluidization processes as hydraulic classification is a comparatively new method and comprises a column in which water and solids are brought into contact. The current of water moves upwards while the solid particles move downwards and/or upwards depending on the difference in their size and density. The separation devices such as teeter bed separators, Stoke's hydrosizer, floatex density separator, cross-flow separator and reflux classifiers are included in the category of fluidized bed classifiers (Galvin et al., 1999; Tripathy et al., 2015).

In fluidization, phenomena such as dispersion, segregation, fluctuation velocity, interstitial fluid velocity, layer inversion and slip velocity are the main areas of research interests among many researchers (Dorgelo et al., 1985; Asif and Petersen, 1993; Galvin et al., 2006; Peng et al., 2016; Abbasfard et al., 2018; Khan et al., 2017; Syed et al., 2018; Khan et al., 2019). The phenomenon of dispersion or diffusion, however, remains the most critical area to understand the hydrodynamics of fluidized beds. In this regard, Kennedy and Bretton (1966) were the first to propose a segregation-dispersion model to characterize the hydrodynamics of fluidized bed separators. According to the authors, solid particle transport in a fluidized bed has a combined effect of two counteracting mechanisms, i.e. the dispersion

and segregation fluxes. Dispersion refers to the intermixing tendency of solid particles within a liquid fluidized bed (Kennedy and Bretton, 1966; Galvin et al., 2006) and tends to disperse solid particles uniformly during a fluidization process. If there is no dispersion, complete segregation of solid particles could be possible. Kennedy and Bretton (1966) applied Fick's law of diffusion to describe the one-dimensional self-diffusion of particle species in fluidized beds. According to the Fick's Law, the diffusion or dispersion flux of solid particles in a fluidized bed is quantified as the product of concentration gradient and the dispersion coefficient, D , (Bird et al., 1960; Kennedy and Bretton, 1966; Juma and Richardson, 1983).

Subsequently, several semi-empirical, theoretical and computational correlations were proposed to quantify the dispersion coefficient of solid particles. Van der Meer et al. (1984) proposed a correlation that showed the dependency of the dispersion coefficient, D , of solid particles on the liquid superficial velocity, v_{sf} , given as:

$$D_i = 0.25 v_{sf}^{2.2} \quad (1)$$

The above correlation was modified by Dorgelo et al. (1985) as:

$$D_i = 0.1 v_{sf}^2 \quad (2)$$

In another study, Batchelor (1988) developed a theoretical correlation stating that the dispersion coefficient of solid particles also depends on particle diameter, d_p , and local liquid volume fraction or voidage, ϕ_f . Similarly, Kang et al. (1990) proposed an equation showing that the D depends on the superficial velocity of the liquid and the minimum fluidization velocity, v_{mf} , given as:

$$D_i = 2.97 \times 10^{-3} (v_{sf} + v_{mf})^{0.802} \quad (3)$$

Nonetheless, the above correlations did not consider the effects of other properties of fluid and particles, such as interstitial fluid velocity, suspension density and particle density, which reduced the applicability of those correlations (Asif and Petersen, 1993). Asif and Petersen (1993) suggested a more generalized correlation based on dimensionless parameters, Froude Number, Fr , and Peclet Number, Pe to properly describe, on a broader scale, the influence of the properties of particles and fluid on the D . The correlation by Asif and Petersen (1993) was given as,

$$\frac{Fr}{Pe} = 7.9 \left(\frac{v_{sf} - v_{mf}}{v_t} \right)^{2.141} \quad (4)$$

The authors (Asif and Petersen, 1993) obtained the value of Pe by trial and error method that provided the diffusion coefficients with a better fit to their experimental results. Hence, their assumption of using fixed values of Pe was implicitly validated by finding an agreement between the theory and experiments. Galvin et al. (2006) developed a new comprehensive correlation for D based on the kinetic theory of gases. Such an approach was proposed previously by Gidaspow (1994) to explain the dispersion coefficient of gas molecules in an ideal gas. According to Galvin et al. (2006) the particle dispersion coefficient can be quantified using the following correlation,

$$D_i = \frac{\alpha d_p v_f}{\phi_t} \quad (5)$$

where α , v_f , d_p and ϕ_t are the constant, interstitial fluid velocity, particle diameter and total solid volume fraction, respectively. Eq. (5) states that the dispersion coefficient varies according to local changes in the interstitial fluid velocity and the total solid volume fraction throughout the fluidized bed. The authors provided a detailed comparison of the predictive capabilities of their correlation with other available correlations and described the evaluation of the dispersion coefficient for a narrow range of particle species in terms of size and density over a broad range of fluidization velocities (Galvin et al., 2006; Patel et al., 2008). Similarly, Khan et al. (2017) studied the influence of energy dissipation on the dispersion coefficient and stated that the dispersion coefficient increases with increasing energy dissipation rate, whereas, the energy dissipation rate depends on the liquid superficial velocity.

Many researchers also used fixed values of the dispersion coefficient as a fitting parameter to validate their model predictions with the experimental results (Kennedy and Bretton, 1966; Ramirez and Galvin, 2005; Syed et al., 2018; Syed and Khan, 2019). For instance, Juma and Richardson (1983) used fixed values of the dispersion coefficient, 0.0018 and 0.0028 m^2/s , to obtain the best fit for the predicted concentration profiles. Similarly, Ramirez and Galvin (2005) used a fixed value of dispersion

coefficient, $0.00060 \text{ m}^2/\text{s}$, in their study. Likewise, Syed et al. (2018, 2019) also used fixed values of the dispersion coefficient, $0.00030 \text{ m}^2/\text{s}$, for multicomponent mixtures in the reflux classifier.

The literature related to dispersion in fluidization processes mainly focused on quantifying the value of the dispersion coefficient, predicting the concentration profiles and size distribution of solid particles within fluidized beds (Juma and Richardson, 1983; Patel et al., 2008; Khan et al., 2017). However, the study shows that the majority of the work mainly focused on liquid fluidized beds consisting of mono and binary systems under batch process conditions. Describing the hydrodynamics of the fluidization processes becomes even more difficult when dealing with multicomponent mixtures having dissimilar densities and size at the same time under continuous processing conditions. These processes represent practical applications and their studies are important steps in the direction of the appropriate design and scale up of such processes (Asif, 1997; Syed et al., 2019).

Syed et al. (2018) proposed for the first time a 2D segregation-dispersion model to study multicomponent mixtures under continuous process conditions in the Reflux Classifier (RC). The RC consists of a fluidization and an inclined section (Galvin et al., 2005), Fig. 1. The separation of solid particles in the fluidization section occurs similar to the liquid fluidized beds, however, within the inclined section a set of parallel inclined channels are present that act as efficient classification zones for the device. The inclined channels provide a large settling area to the solid particles during a fluidization process and allow the denser or coarser solid particles to settle at a higher rate as compared to the vertical section. The solid particles after settling on the inclined channels slide backwards and discharge from the base of the RC. A detailed working principle of the device has been provided by Galvin et al. (2010). Syed et al. (2018) modeled the RC with narrow-spaced channels and validated the model predictions with the experimental results of Galvin et al. (2010). The model predictions successfully demonstrated density-based separation and the mechanism of shear-induced lift. The authors used fixed values of the dispersion coefficient, 0.00030 and $0.000030 \text{ m}^2/\text{s}$, in the fluidization and inclined sections of the RC, as fitting parameters. Similarly, in another study focusing on the size classification by Syed et al. (2019), the 2D segregation-dispersion model was utilized to model a multi-size RC with wide channel spacing. In that study, the solid particles had different sizes, but the same density and the separation was based on the differences in the particle size. The value of the dispersion coefficient was kept at $0.00030 \text{ m}^2/\text{s}$ inside the fluidization and inclined sections of the RC.

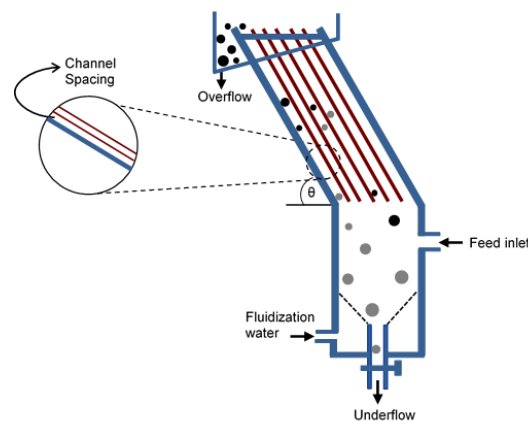


Fig. 1. Schematic representation of a continuous process in the Reflux Classifier

The present study is an extension of Syed et al. (2016) work in which the authors demonstrated density-based separation in the RC with wide channel spacing using the 2D segregation-dispersion model under continuous processing conditions and the effect of shear-induced lift was switched off. A relatively higher value of dispersion coefficient, $0.0030 \text{ m}^2/\text{s}$, was used in the fluidization section as a fixed parameter and the model predictions were validated with the experimental results of Galvin et al. (2005). In this paper, the main focus is to demonstrate the selection of a suitable dispersion coefficient value as a fixed parameter and to illustrate the effects of the dispersion coefficient on the internal state, i.e. separation density, D_{50} , and separation efficiency, E_p , of a multicomponent mixture in the RC using the 2D segregation-dispersion model. Moreover, the correlation of dispersion proposed by Galvin et al.

(2006) was incorporated in the 2D segregation-dispersion and the results obtained were compared with the validated model predictions. Furthermore, the effect of dispersion coefficient on the total solid volume fraction within the fluidized and inclined sections of the RC has been demonstrated. The study is valuable in understanding the effects of the dispersion coefficient on the hydrodynamics of a multicomponent mixture under continuous process conditions. It also provides a basis for developing a new dispersion model that could accurately describe the hydrodynamics of fluidized bed separators under continuous process conditions. The study also emphasized in the application of the 2D segregation-dispersion model that acts as a framework in which different new models could be incorporated and studied.

2. Computational model

The 2D segregation-dispersion model is based on the Kennedy and Bretton (1966) approach and describes the net flux of a solid particle species as a combined effect of dispersion and segregation fluxes at any location within a fluidized vessel and has x and y components (Syed et al., 2018) given as:

$$N_{x,i} = \phi_i v_{p-x,i} = -D_{x,i} \frac{\partial \phi_i}{\partial x} + \phi_i v_{sg-x,i} \quad (6)$$

$$N_{y,i} = \phi_i v_{p-y,i} = -D_{y,i} \frac{\partial \phi_i}{\partial y} + \phi_i v_{sg-y,i} \quad (7)$$

where N_x , N_y , v_{p-x} , v_{p-y} , v_{sg-x} , v_{sg-y} , D_x , D_y , ϕ_i are the x and y components of net flux, particle velocity, segregation velocity relative to the vessel, dispersion coefficient and the solid volume fraction, respectively. Similarly, $-D_i \frac{\partial \phi_i}{\partial x}$ and $-D_i \frac{\partial \phi_i}{\partial y}$ are the dispersion fluxes in the x and y directions, whereas $\phi_i v_{sg-x,i}$ and $\phi_i v_{sg-y,i}$ are the segregation fluxes in the x and y directions of the solid particle species i , respectively.

The total volume flux, v_n , comprising solids and liquid, just above the feed inlet can be represented mathematically as (Syed et al., 2018):

$$v_n = v_{fs} + N_f - N_u = v_f \phi_f + \sum \phi_i v_{p,i} \quad (8)$$

In the same way, the total volume flux below the feed point is given as:

$$v_n = v_{fs} - N_u = v_f \phi_f + \sum \phi_i v_{p,i} \quad (9)$$

where, v_{fs} , v_f , N_f , N_u and ϕ_f are the superficial fluidization velocity, interstitial fluid velocity, feed flux, underflow flux and voidage, respectively.

The complete algorithm of the 2D segregation-dispersion model can be seen in Syed et al. (2018) article. However, a brief description of the incorporation of the hindered settling model has been provided here.

The x and y components of the segregation velocity in Eq. (10 & 11) are quantified as a sum of the particle slip relative to the fluid and interstitial fluid velocities, given as:

$$v_{seg-x,i} = v_{slip-x,i} + v_{f-x} \quad (10)$$

$$v_{seg-y,i} = v_{slip-y,i} + v_{f-y} \quad (11)$$

where $v_{slip-x,i}$ and $v_{slip-y,i}$ are the x and y components of slip velocities, respectively. While, v_{f-x} and v_{f-y} are the interstitial fluid velocities in the x and y directions, respectively.

The slip velocity was calculated by incorporating the hindered settling model of Asif (1997). A directional parameter, ℓ , was also introduced to define the motion of solid particle species in the upward and downward directions (Syed et al., 2016, 2018). The slip velocity model with its x and y components is given as:

$$v_{slip-x,i} = \left[v_{t,i} \ell \left| \left(\frac{\rho_i - \rho_{sus}}{\rho_i - \rho_f} \right) \right|^{n_i-1} \right] \cos\theta \quad (12)$$

$$v_{slip-y,i} = \left[v_{t,i} \ell \left| \left(\frac{\rho_i - \rho_{sus}}{\rho_i - \rho_f} \right) \right|^{n_i-1} \right] \sin\theta \quad (13)$$

where ρ_i is the density of solid particles, ρ_f is the density of the fluid, ρ_{sus} is the suspension density and v_t is the particle terminal velocity. The suspension density is given as:

$$\rho_{sus} = \sum \phi_i \rho_i + (1 - \sum \phi_i) \rho_f \quad (14)$$

A fixed value of the Richardson and Zaki (1954) exponent n , i.e. 3.2, was considered as a fitting parameter (Syed et al. 2018). The particle terminal settling velocity was calculated as:

$$Re_t = \frac{\rho_f v_t d_p}{\mu_f} \quad (15)$$

To calculate the particle Reynolds number, Re_t , the equation of Zigrang and Sylvester (1981) was utilized:

$$Re_t = \left[(14.51 + 1.83(g \times (\rho_i - \rho_f) \rho_f)^{0.5} \frac{d^{1.5}}{\mu_f})^{0.5} - 3.81 \right]^2 \quad (16)$$

where μ_f is the viscosity of the fluid and g is the gravitational constant.

2.1. Simulation parameters

Simulations were performed on a system 2.0 m in height with fluidization and inclined sections, each having a length equal to 1 m. The cross-sectional area of the computational domain was 0.0060×0.0060 m². The whole system was divided into 11 elements and 100 shells in the x and y directions, respectively. Element 1 was the nearest element to the upward-facing wall of the inclined channel, element 6 was the middle region and element 21 was nearer to the upper surface of the inclined channel (Syed et al., 2016, 2018). The feed inlet point was taken at a height of 0.7 m (shell 35) within the fluidization section.

The feed consisted of a multicomponent mixture comprising total of 35 types of solid particle species with five different sizes and seven different densities at the same time. The average particle size, 1.70, 1.20, 0.85, 0.60 and 0.35 mm, was selected in a way to represent the particle size range -2.0+1.40, -1.40+1.0, -1.0+0.70, -0.70+0.50 and -0.50+0.25 mm, respectively, as used by Galvin et al. (2005). The particle size selection, e.g. -2.0+1.40 mm, illustrated that the material passed through a screen size -2.0 mm while was retained on the screen size +1.40 mm.

A feed (slurry) flux of 0.016 m³/m²s (67.2 t/m²h) containing total solid flux of 0.0040 m³/m²s (24.0 t/m²h) and water flux of 0.012 m³/m²s (43.2 t/m²h) was introduced into the system. The fluidization velocity and underflow rate were selected equal to 0.0050 m³/m²s and 0.0040 m³/m²s, respectively, to attain a separation density value (density cut point) according to the experimental conditions of Galvin et al. (2005). The properties of the solid particles are shown in Table 1.

2.2. Methodology

Several simulation runs were performed under continuous process conditions using the 2D segregation-dispersion model for different values of the dispersion coefficient. Table 2 shows worth mentioning simulation runs, Run 1-5, whose results are discussed in this paper. Fixed values of the dispersion coefficient were considered in Run 1-4 as a fitting parameter both in the y (parallel to the plane) and the x (normal to the plane) directions within the computational domain of the RC (Syed et al., 2016 2018). In each run, the value of the dispersion coefficient was changed while all other process conditions were kept constant. Furthermore, in Run 5, the dispersion correlation proposed by Galvin et al. (2006) was incorporated in the 2D model and its results were examined. The data generated through simulations were used to produce partition curves from which the corresponding values of the separation density, D_{50} , and separation efficiency or Ecart probable error, Ep , were derived. Some partition curves and extra simulation results are shown in Appendix I & II. The D_{50} value is the density cut point and represents the solid particle species that have a 50% probability to move out from the system either via the overflow or the underflow. The Ep value defines the separation quality of a device. If the value of Ep is near to zero, it depicts good separation quality, whereas, if the Ep value is near to one, it exhibits poor separation quality.

3. Results and discussion

3.1. Effect of the dispersion coefficient on the separation density

Simulations were performed using different values of the dispersion coefficient, Table 2. The predictive values of D_{50} obtained for Run 1, in which a relatively higher value of the dispersion coefficient, 0.0030

Table 1. Properties of the solid particles used in simulations

Particle size (mm)	Particle density (kg/m ³)	Particle Reynolds number	Terminal velocity (m/s)
1.70	1400	158.1	0.093
1.70	1500	181.3	0.106
1.70	1600	202.6	0.119
1.70	1700	222.3	0.130
1.70	1800	240.9	0.142
1.70	1900	258.4	0.152
1.70	2000	275.1	0.161
1.20	1400	81.7	0.068
1.20	1500	94.4	0.079
1.20	1600	106.0	0.088
1.20	1700	116.9	0.097
1.20	1800	127.1	0.106
1.20	1900	136.8	0.114
1.20	2000	146.0	0.122
0.85	1400	41.0	0.048
0.85	1500	47.7	0.056
0.85	1600	54.0	0.064
0.85	1700	59.8	0.070
0.85	1800	65.4	0.077
0.85	1900	70.6	0.083
0.85	2000	75.7	0.089
0.60	1400	19.6	0.033
0.60	1500	23.0	0.038
0.60	1600	26.2	0.044
0.60	1700	29.2	0.049
0.60	1800	32.1	0.054
0.60	1900	34.9	0.058
0.60	2000	37.5	0.063
0.35	1400	5.6	0.016
0.35	1500	6.7	0.019
0.35	1600	7.8	0.022
0.35	1700	8.8	0.025
0.35	1800	9.8	0.028
0.35	1900	10.7	0.031
0.35	2000	11.6	0.033

m²/s, and a value equal to 0.00030 m²/s, in the fluidization and inclined sections, respectively, were used, agreed well with the experimental results of Galvin et al. (2005) (Syed et al., 2016, Fig. 7), tabulated in Table 3. However, slight differences were observed in the D₅₀ values for the finer species. The value of the D₅₀ for the finer species, 0.35 mm, obtained from the model predictions was 2.03 as compared to the experimental results for which the D₅₀ value for the corresponding size was 1.94. A higher value of D₅₀ for finer species showed that all the fine solid particles moved out from the RC via the overflow because the largest density used in the simulations was 2000 kg/m³. In contrast, the value of D₅₀ for the coarser species, 1.70 mm, was 1.46 in the experiments (Galvin et al., 2005), whereas the model predicted it equal to 1.45. The lowest density used in the simulations was 1400 kg/m³, which shows that the maximum amount of coarser solid particles discharged from the base of the system.

Fig. 2a, b shows model predictions for Run 1-5 demonstrating the D₅₀ value as a function of particle size under steady-state conditions. In order to show clarity, the validated predictions of Run 1 are also shown separately in Fig. 2a. The model predictions exhibited a monotonic decrease in the D₅₀ values

with increasing particle size as was observed experimentally by Galvin et al. (2005). Fig. 2b shows a comparison of the validated predictions of Run 1 with the model predictions of Run 2-5. The comparison showed minor differences in the D_{50} values for all the runs, however, in Run 4, the value of D_{50} for the finer species was 2.20 providing a large difference with the validated predictions. Furthermore, in Run 5, the D_{50} values accurately matched with the validated predictions for the average particle sizes 1.70, 1.20, and 0.60 mm. However, slight discrepancies existed in the D_{50} values for the particle sizes 0.85 and 0.35 mm. Nevertheless, the most important feature of the results was that the differences in the D_{50} values were not significant. This illustrated that the dispersion coefficient did not affect much the D_{50} values within the range of values studied.

Table 2. Simulation runs with different values of the dispersion coefficient

Simulation runs	Dispersion coefficient (m^2/s)	
	Fluidization section	Inclined channel
Run1 - Validated Predictions		
x - direction	0.0030	0.00030
y - direction	0.0030	0.00030
Run 2 - Predictions		
x - direction	0.00030	0.000030
y - direction	0.00030	0.000030
Run 3 - Predictions		
x - direction	0.00030	0.00030
y - direction	0.00030	0.00030
Run 4 - Predictions		
x - direction	0.0030	0.0030
y - direction	0.0030	0.0030
Run 5 - Predictions		
Dispersion Model (Galvin et al. 2006)	$D_i = \frac{\alpha d_p u_f}{\phi_t}$	$D_i = \frac{\alpha d_p u_f}{\phi_t}$

Table 3. The separation density, D_{50} , values

Particle size (mm)	Validated predictions of Run 1	Experimental values by Galvin et al. (2005)
1.70	1.45	1.46
1.20	1.51	1.53
0.85	1.59	1.61
0.60	1.73	1.74
0.35	2.03	1.94

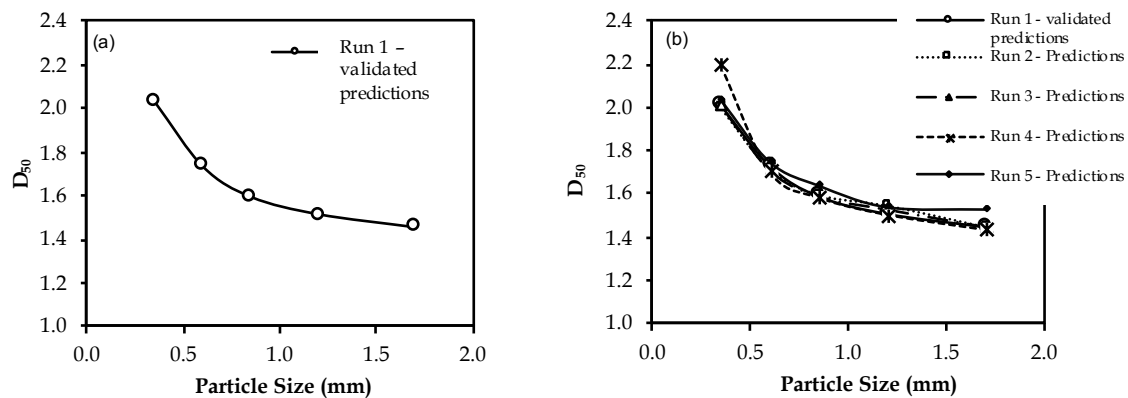


Fig. 2. The separation density, D_{50} , as a function of particle size: (a) The D_{50} versus particle size for the validated predictions Run 1, (b) A comparison of validated predictions with the simulation runs i.e. Run 2-5

3.2. Effect of the dispersion coefficient on the separation efficiency

The values of separation efficiency, E_p , were derived from the corresponding partition curves of Run 1-5. Table 4 provides a comparison of the validated E_p values of Run 1 with the experimental results of Galvin et al. (2005). The E_p values of Run 1 gave a very good agreement with the experimental results.

Fig. 3 shows E_p as a function of particle size under steady-state conditions and provides a comparison between the validated model predictions of Run 1 and the model predictions for Run 2-5. In Fig. 3, the curve with empty circles represents the validated model predictions and depicts that the E_p values decreased monotonically with increasing particle size following the same pattern as was observed experimentally by Galvin et al. (2005). The figure shows that the separation quality for finer species, 0.35 mm, was poor due to a higher value of E_p , 0.13. In contrast, the E_p value of the coarser species, 1.70 mm, was 0.022 showing a good separation quality.

Table 4. The separation efficiency, E_p , values

Particle size (mm)	Validated predictions of Run 1	Experimental values by Galvin et al. (2005)
1.70	0.022	0.025
1.20	0.036	0.040
0.85	0.050	0.052
0.60	0.073	0.075
0.35	0.13	0.12

The comparison of E_p values in Fig. 3 illustrates that the E_p values differed significantly with changes in the values of the dispersion coefficient. As discussed, the best agreement was obtained for Run 1 (curve with empty circles) in which the values of the dispersion coefficient in the fluidization and inclined sections were kept constant at 0.0030 and 0.00030 m^2/s , respectively. The first important effect to observe was that the curve corresponding to Run 4 (curve with asterisk) was relatively close to the curve corresponding to the validated model predictions of Run 1. These two curves were obtained for the same values of the dispersion coefficient, 0.0030 m^2/s , in the fluidization section, but different values in the inclined section (Table 2). A higher value of the dispersion coefficient in the fluidization section provided higher values of E_p demonstrating that the separation was not fine in that region. This indicates that the tendency of intermixing of solid particles was higher in the fluidization section of the RC than in the inclined section. This might be due to the fact that there were probably two major points where the intermixing tendency of solid particles was high, one at the feed inlet and second at the junction of the fluidization and inclined sections due to the reflux action of the device. This fact was further corroborated by comparing the large differences observed between the E_p values of Run 2 and Run 3 with the validated model predictions in which lower values of the dispersion coefficient, 0.00030 m^2/s , were kept in the fluidization section and hence lower E_p values were obtained.

Moreover, the values of the E_p predicted using the correlation of the dispersion coefficient (Run 5) proposed by Galvin et al. (2006) also demonstrated a significant reduction in the E_p values with increasing particle size over a small range of particle size (0.30 and 0.85 mm). In addition, the corresponding values of the E_p were much lower and hence a significant difference in the validated model predictions and Run 5 was observed. Nevertheless, the correlation of the dispersion coefficient proposed by Galvin et al. (2006) was able to predict a monotonic reduction in the values of the D_{50} and E_p with increasing particle size, although it could not be used to validate the model predictions with Run 1 and the experimental results.

The above illustrations show that the dispersion coefficient had a higher influence on the separation efficiency of the reflux classifier. As dispersion is an opposing phenomenon during the particle transport in a fluidized bed separator or hydrosizer, so, a higher value of the dispersion coefficient will reduce the separation efficiency of the device and vice versa. The above study also shows that a new correlation of dispersion coefficient by considering the effect of superficial velocity at the feed inlet could be proposed. Such a correlation would be capable of predicting the dispersion of solid particles in a continuous fluidization process.

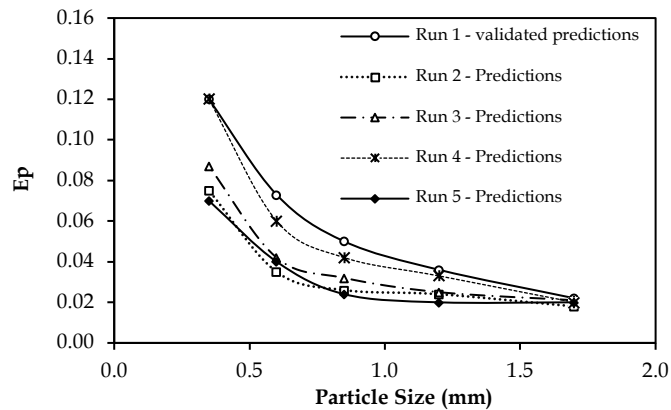


Fig. 3. A comparison of validated predictions of Run 1 with the simulations runs i.e. Run 2-5, demonstrating the pattern of decrease in the separation efficiency or Ecart probable error, E_p , values with increasing particle size

3.3. Effect of the dispersion coefficient on the total solid volume fraction

Fig. 4a, b, c demonstrates the effect of the dispersion coefficient on the total solid volume fraction for the simulation runs (Run 1-4) in element 1, 6 and 11. The figure shows two main sections, the fluidization and inclined sections within the reflux classifier. Additionally, two distinct zones within the fluidization section of the reflux classifier are illustrated, first a higher concentration zone from feed inlet to the base and second a dilute zone above the feed inlet and below the inclined section of the device.

Fig. 4a shows a comparison of the total solid volume fractions versus height for the four simulation runs, Run 1 – 4, in element 1. The validated predictions of Run 1, show that the total solid volume fraction in element 1 had a maximum solid volume fraction of 0.60 near the base and it decreased to a value of 0.47 at a height of 0.60 m, near the feed inlet, within the fluidization section. It further decreased to a value of 0.36 in the dilute zone. In the inclined channel, the total solid volume fraction had a maximum value of 0.37 approximately, along the channel length. In contrast, the plot of Run 2 shows that when the values of the dispersion coefficient were 0.00030 and 0.000030 m^2/s in the fluidization and inclined sections of the device, respectively, the system achieved a maximum total solid volume fraction of 0.57 near the base. The total solid volume fraction decreased a bit up to the height of 0.20 m and then maintain a constant value of 0.57 to a height of 0.60 m, whereas, it started to decrease and reached a value of 0.37 in the dilute zone. In the inclined section, there was a significant increase in the total solid volume fraction for the Run 2 and reached a maximum value of 0.50. This illustrates that within the inclined section, due to a lower value of the dispersion coefficient, the solid particles settled at a higher rate and hence the volume fraction of the solid particles increased.

The model predictions for Run 3 show that the total solid volume fraction illustrated a behavior identical to Run 2 within the fluidization section, whereas, a similar trend of the solid volume fraction of Run 1 within the inclined channel. This was understandable as the dispersion coefficient values were 0.00030 m^2/s in both the fluidization and inclined sections of the RC. In Run 4, a relatively higher value of dispersion coefficient, 0.0030 m^2/s , was selected in both the fluidization and inclined sections of the RC. The total solid volume fraction showed a similar trend as of Run 1 in the fluidization section of the RC. However, within the inclined channel, it reached a maximum value of 0.35, comparatively lower than the total solid volume fractions of the three simulation runs studied here.

Fig. 4b, c demonstrates the total solid volume fraction versus height in elements 6 and 11. The model predictions show that the total solid volume fraction decreased in element 6 and 11 for the simulation Runs 1 and 3. Moreover, a significant reduction in the total solid volume fraction was observed in element 6 and 11 for Run 3. In Run 3, due to a lower value of the dispersion coefficient, the solid particles settled at a higher rate and thus the total solid volume fraction decreased to a lower value of 0.12 in element 11. In contrast, the behavior of the system was different when a higher value of the dispersion coefficient was used in Run 4. In that case (Run 4), the total solid volume fraction almost remained the same in all the elements, showing that the solid particles were mostly suspended due to the higher dispersion or intermixing effect.

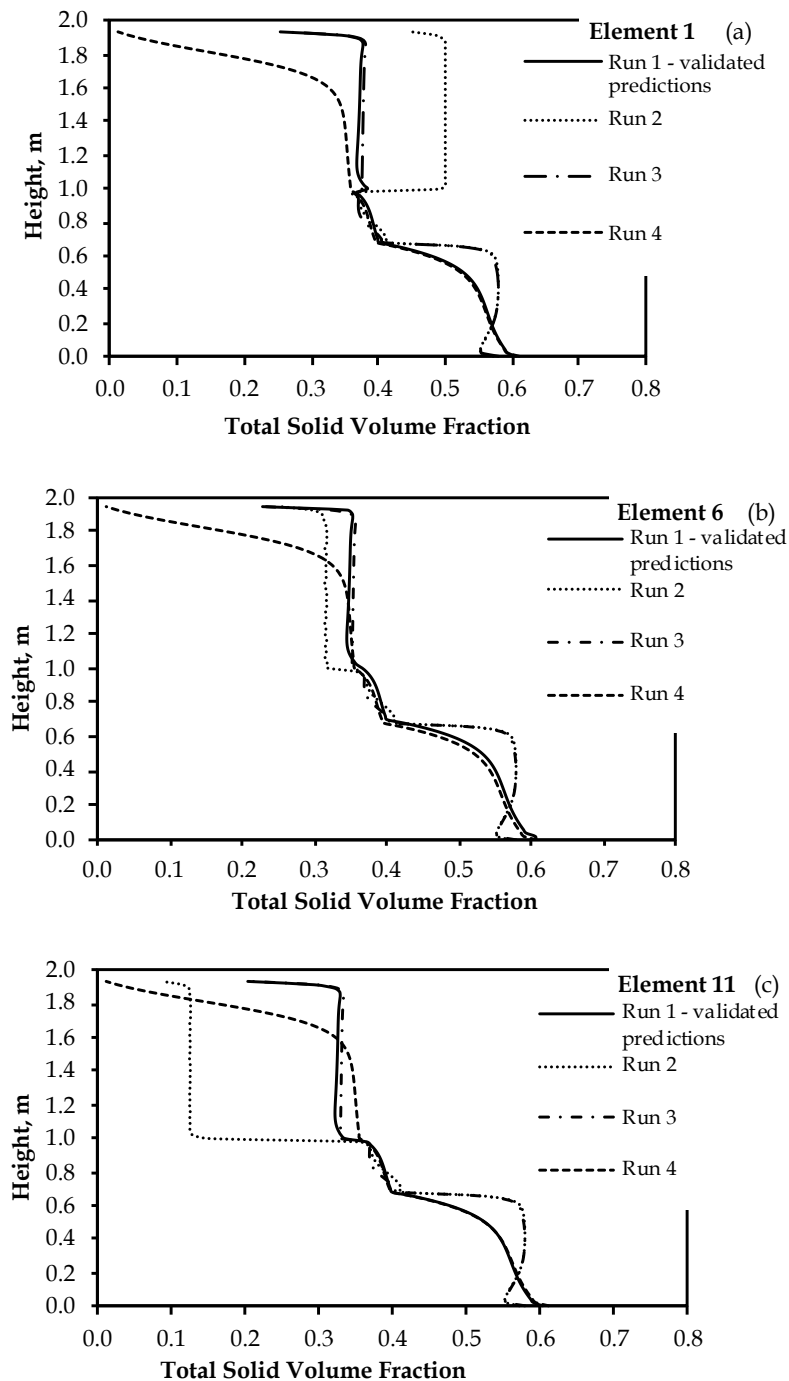


Fig. 4. Total solid volume fraction versus height for the simulations Runs 1, 2, 3, and 4: (a) Total solid volume fraction versus height in element 1, (b) Total solid volume fraction versus height in element 6, (c) Total solid volume fraction versus height in element 11

4. Conclusions

A 2D continuous segregation-dispersion model was used to examine the effect of dispersion coefficient on the internal state of a multicomponent mixture in the Reflux Classifier (RC) with wide channel spacing. Simulations were performed for five different runs, Run 1-5, under continuous processing conditions with changed values of the dispersion coefficient and their effects on the D_{50} , E_p , and total solid volume fraction was studied. The model predictions provided a good agreement for Run 1 in which the values of the dispersion coefficient were kept constant at 0.0030 and 0.00030 m^2/s , in the fluidization and inclined sections of the RC, respectively. The simulation results of the other four runs, Run 2-5, were compared with the validated predictions of the model. It was observed that different

values of the dispersion coefficient had not much effect on the D_{50} values. In contrast, the values of E_p showed significant variations with the changing dispersion coefficient values. The smaller values of the dispersion coefficient provided lower values of the E_p that did not match well with the validated predictions, nevertheless, the lower values of the dispersion coefficient caused good separation quality.

Furthermore, the variations in the total solid volume fraction for different values of the dispersion coefficient was also demonstrated by plotting concentration profiles versus height. It was found that at a higher value of the dispersion coefficient, $0.0030 \text{ m}^2/\text{s}$, in the inclined section, the model predictions exhibited no change in the values of the total solid volume fraction, Fig. 4, revealing that the solid particles were in suspended form. On the other hand, a lower value of the dispersion coefficient, $0.000030 \text{ m}^2/\text{s}$, showed a higher settling rate of solid particles, Fig 4c, that resulted in smaller values of the total solid volume fraction within the inclined section. The pattern of the total solid volume fraction of the validated predictions was, however, considered more suitable.

Acknowledgments

The authors greatly acknowledge the facilities and funding provided by the Department of Chemical Engineering, University of Engineering & Technology Peshawar, Pakistan during this research work.

Nomenclature

D	dispersion coefficient (m^2/s)	Greek letters	
N	net flux ($\text{m}^3/\text{m}^2\text{s}$)	ϕ	solid volume fraction
N_f	feed flux ($\text{m}^3/\text{m}^2\text{s}$)	ϕ_f	voidage
N_u	underflow flux ($\text{m}^3/\text{m}^2\text{s}$)	μ	fluid viscosity (Pa s)
n	Richardson Zaki exponent (dimensionless)	ρ_f	liquid density (kg/m^3)
Re_t	particle Reynolds number (dimensionless)	ρ	particle density (kg/m^3)
v_{fs}	superficial fluidization velocity (m/s)	ρ_{sus}	suspension density (kg/m^3)
v_f	interstitial fluid velocity (m/s)	Subscripts	
v_p	particle velocity (m/s)	sg	segregation
v_{sg}	segregation velocity of solid particles (m/s)	f	liquid fluid
v_t	terminal settling velocity of solid particles (m/s)	i	ith particle
v_n	total volume flux (m/s)	sus	suspension
v_{slip}	slip velocity of solid particles (m/s)		

Appendix - I

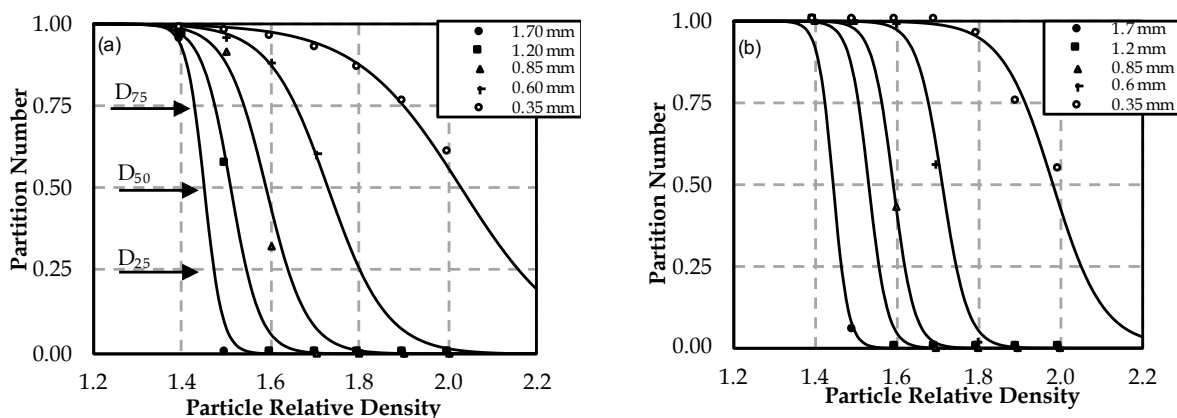


Fig. A1. Partition curves obtained from the data generated through simulations demonstrating the probability of solid particle species to report either as overflow or underflow: (a) Run 1, (b) Run 2

$$\text{Separation efficiency or Ecart probable error, } E_p, \text{ was obtained as: } E_p = \frac{D_{25} - D_{75}}{2} \quad (\text{A1})$$

Appendix - II

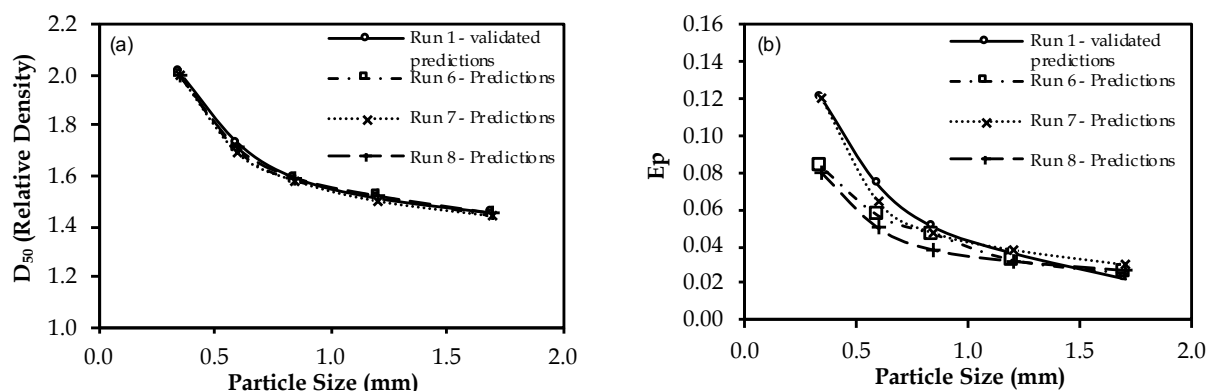


Fig. A2. Comparison of extra simulation runs, 6, 7 and 8, with Run 1: (a) D_{50} versus particle size, (b) E_p versus particle size

Table A1. Extra simulation runs with different dispersion coefficient values.

Simulation runs	Planes	D in Fluidization section (m^2/s)	D in Inclined channel (m^2/s)
Run 6 - Predictions	x - direction	0.00030	0.0030
	y - direction	0.00030	0.00030
Run 7 - Predictions	x - direction	0.00030	0.00030
	y - direction	0.0030	0.0030
Run 8 - Predictions	x - direction	0.0030	0.030
	y - direction	0.0030	0.0030

References

- ABBASFARD, H., EVANS, G.M., KHAN, M.S., MORENO-ATANASIO, R., 2018. *A new two-phase coupling model using a random fluid fluctuating velocity: application to liquid fluidized beds*. Chemical Engineering Science, 180, 79-94.
- ASIF, M., 1997. *Modeling of multi-solid liquid fluidized beds*. Chemical Engineering Technology, 20, 485-490.
- ASIF, M., and PETERSEN, J.N., 1993. *Particle dispersion in a binary solid-liquid fluidized bed*. A.I.Ch.E. Journal, 39 (9), 1465-1471.
- BATCHELOR, G.K., 1988. *A new theory of the stability of a uniform fluidized bed*. Journal of Fluid Mechanics, 193, 75-110.
- BIRD, R. B., STEWART, W. E., LIGHTFOOT, E. N., 1960. *Transport phenomena*. New York: Wiley.
- Di FELICE, R., 1995. *Hydrodynamics of liquid Fluidization*. Chemical Engineering Science, 50, 1213-1245.
- DORGELO, E. A. H., VAN DER MEER, A. P., WESSELINGH, J.A., 1985. *Measurement of the axial dispersion of Particles in a liquid Fluidized bed applying random walk model*. Chemical Engineering Science, 40, 2105-2111.
- GALVIN, K.P., CALLEN, A., ZHOU, J., DOROODCHI, E., 2005. *Performance of the reflux classifier for gravity separation at full scale*. Minerals Engineering, 18, 19-24.
- GALVIN, K.P., PRATTEN, S.J., NICOL, S.K., 1999. *Dense medium separation using a teetered bed separator*. Minerals Engineering, 12, No. 9, 1059-1081.
- GALVIN, K.P., SWANN, R., RAMIREZ, W.F., 2006. *Segregation and dispersion of a binary system of particles in a Fluidized bed*. AIChE journal, 52, 3401-3410.
- GALVIN, K.P., ZHOU, J., WALTON, K., 2010. *Application of closely spaced inclined channels in gravity separation of fine particles*. Minerals Engineering, 23, 326-338.
- GIDASPOW, D., 1994. *Multiphase Flow and Fluidization: Continuum and Kinetic Theory Descriptions*. Academic Press, San Diego, CA.
- JUMA, A. K. A., and RICHARDSON, J. F., 1983. *Segregation and mixing in liquid fluidized beds*. Chemical Engineering Science, 38 (6), 955-967.

- KANG, Y., NAH, J.B., MIN, B.T., KIM, S.D., 1990. *Dispersion and fluctuation of Fluidized particles in a liquid-solid fluidized bed*. Chemical Engineering Communication, 97, 197-208.
- KENNEDY, S.C., BRETTON, R.H., 1966. *Axial dispersion of spheres fluidized with liquids*. AIChE Journal, 12, 24-30.
- KHAN, M.S., EVANS, G.M., NGUYEN, A.V., MITRA, S., 2019. *Analysis of particle dispersion coefficient in solid-liquid fluidized beds*. Powder Technology, In Press.
- KHAN, M.S., MITRA, S., GHATAGE, S.V., DOROODCHI, E., JOSHI, J.B., EVANS, G.M., 2017. *Segregation and dispersion studies in binary solid-liquid fluidized beds: a theoretical and computational study*. Powder Technology, 314, 400-411.
- PATEL, B.K., RAMIREZ, W.F., GALVIN, K.P., 2008. *A generalized segregation and dispersion model for liquid fluidized beds*. Chemical Engineering Science, 63, 1415-1427.
- PENG, Z., JOSHI, J.B., MOGHADERI, B., KHAN, M.S., DOROODCHI, E., EVANS, G.M., 2016. *Segregation and Dispersion of Binary Solids in Liquid Fluidized Beds: a CFD-DEM Study*. Chemical Engineering Science, 152, 65-83.
- RAMIREZ, W.F., GALVIN, K.P., 2005. *Dynamic model of multi-species segregation and dispersion in fluidized beds*. AIChE journal, 51, 2103-2108.
- RICHARDSON, J.F., and ZAKI, W.N., 1954. *Sedimentation and fluidization: Part I*. Transactions of the Institution of Chemical Engineers, 32, 35-53.
- SYED, N.H., DICKINSON, J.E., GALVIN, K.P., MORENO-ATANASIO, R., 2018. *Continuous, dynamic and steady state simulations of the reflux classifier using a segregation-dispersion model*. Minerals Engineering, 115, 53-67.
- SYED, N.H., GALVIN, K.P., MORENO-ATANASIO, R., 2016. *Segregation-dispersion model of a fluidized bed system incorporating inclined channels operated with no shear induced lift*. Chemical Engineering - Regeneration, Recovery and Reinvention. Melbourne, Vic.: Engineers Australia, 570-580.
- SYED, N.H., GALVIN, K.P., MORENO-ATANASIO, R., 2019. *Application of a segregation-dispersion model to describe binary and multi-component size classification in a Reflux Classifier*. Minerals Engineering, 133, 80-90.
- SYED, N.H., KHAN, N., 2019. *Simulations of mono-sized solid particles in the reflux classifier under continuous process conditions*. Physicochemical Problems of Mineral Processing, 55(3), 631-642.
- TRIPATHY, S.K., BHOJA, S.K., KUMAR, C.R., SURESH, N., 2015. *A short review on hydraulic classification and its development in mineral industry*. Powder Technology, 270, 205-220.
- VAN DER MEER, A. P., BLANCHARD, M. R. J. P., WESSELINGH, J.A., 1984. *Mixing of particles in liquid fluidized beds*. Chemical Engineering Research and Design, 62, 214-222.